Synthesis and Photorefractive Properties of Multifunctional Glasses

Meng He,[†] Robert J. Twieg,*[,†] Ulrich Gubler,[‡] Daniel Wright,[‡] and W. E. Moerner[‡]

Department of Chemistry, Kent State University, Kent, Ohio 44242, and Department of Chemistry, Stanford University, Stanford, California 94305-5080

Received July 1, 2002. Revised Manuscript Received December 30, 2002

A set of organic glasses has been synthesized and evaluated for photorefractive performance. The functions of optical nonlinearity, birefringence, and charge transport were built into a single molecule by attaching an NLO chromophore to a charge transport moiety with an adjustable linking group. The longer linking group not only lowers the glass transition temperature T_g but also influences the photorefractive performance of the samples. The photorefractive gain coefficient is larger for longer linkers with about a 2-fold increase going from the 2-carbon atom linker to 12. The glass stability and chemical stability of the materials was adequate for full photorefractive characterization.

Introduction

Photorefractive (PR) materials combine both photoconductivity and a nonlinear optical response to produce a reversible light-induced modulation of the refractive index.[1] The first unequivocal polymeric PR material was reported in 1991.[2] Relative to inorganic media, organic materials provide greater flexibility for structure modification to meet the diverse requirements for the PR effect.[3,4] Several components (functions) are required in PR materials: a sensitizer (photoionizable charge generator), a charge-transporting medium with trapping sites, and a chromophore with either (or both) a large electro-optic effect or large birefringence.[5] Plasticizers are often added to adjust the glass transition temperature (T_g) of the amorphous composite to around ambient temperature (the most common temperature of study of the photorefractive media). As a typical example of a PR polymer composite, the system consisting of the hole-transporting polymer poly(*N*-vinyl carbazole) (PVK), an aminodicyanostyrene nonlinear optical chromophore (AODCST), C_{60} as a sensitizer, and butyl benzyl phthalate (BBP) as an added plasticizer, produces a large net PR gain coefficient ($\Gamma > 230$ cm^{-1}) and an initial two-wave-mixing response time as fast as 4 ms.[6] Other polymer composite systems reported thus far with interesting performance have photorefractive gain coefficients of $\Gamma \approx 400$ cm^{-1} or more[7] and nearly 100% diffraction efficiencies.[8] Unfortunately, these favorable properties often require large applied electric fields of up to 100 V/μm or occur in samples lacking long-term stability.

There are a variety of ways in which the full range of functional components may be distributed in photorefractive media. The components may be a set of independent discrete molecules or some or all of them may be covalently bound together, thus partially or completely alleviating the problem of phase separation of the various components. It is also possible that a single component may be multifunctional, for example, as in the case where a birefringent chromophore also functions as a charge-transporting agent. The interplay among the different components is complex and simultaneously impacts the electronic, optical, and morphological properties of the composite. Fully functionalized polymers,[9] oligomers,[10] and low-molar-mass glasses[11−14] represent several of the formulation strategies.

* To whom correspondence should be addressed.
[†] Kent State University.
[‡] Stanford University.

(1) Solymar, L.; Webb, D. J.; Grunnet-Jepsen, A. *The Physics and Applications of Photorefractive Materials*; Clarendon Press: Oxford, 1996.
(2) Ducharme, S.; Scott, J. C.; Twieg, R. J.; Moerner, W. E. *Phys. Rev. Lett.* **1991**, *66*, 1846.
(3) Moerner, W. E.; Grunnet-Jepsen, A.; Thompson, C. L. *Annu. Rev. Mater. Sci.* **1997**, *27*, 585.
(4) Zilker, S. *ChemPhysChem* **2000**, *1*, 72.
(5) Moerner, W. E.; Silence, S. M. *Chem. Rev.* **1994**, *94*, 127.
(6) Wright, D.; Diaz-Garcia, M. A.; Casperson, J. D.; DeClue, M.; Moerner, W. E.; Twieg, R. J. *App. Phys. Lett.* **1998**, *73*, 1490.
(7) (a) Wright, D.; Gubler, U.; Roh, Y.; Moerner, W. E.; He, M.; Twieg, R. J. *Appl. Phys. Lett.* **2001**, *79*, 4274. (b) Ostroverkhova, O.; Wright, D.; Gubler, U.; Moerner, W. E.; He, M.; Sastre-Santos, A.; Twieg, R. J. *Adv. Funct. Mater.* **2002**, *12*, 621.
(8) Meerholz, K.; Volodin, B. L.; Sandalphon; Kippelen, B.; Peyghambarian, N. *Nature* **1994**, *371*, 497.
(9) (a) Kippelen, B.; Tamura, K.; Peyghambarian, N.; Padias, A. B.; Hall, H. K., Jr. *Phys. Rev. B* **1993**, *48*, 10710. (b) Bratcher, M. S.; DeClue, M. S.; Grunnet-Jepsen, A.; Wright, D.; Smith, B. R.; Moerner, W. E.; Siegel, J. S. *J. Am. Chem. Soc.* **1998**, *120*, 9680. (c) Wang, Q.; Wang, L.; Yu, J.; Yu, L. *Adv. Mater.* **2000**, *12*, 13, 974. (d) Hattemer, E.; Zentel, R.; Mecher, E.; Meerholz, K. *Macromolecules* **2000**, *33*, 1972. (e) Steenwinckel, D. V.; Hendrickx, E.; Persoons, A. *Chem. Mater.* **2001**, *13*, 1230.
(10) (a) Ng, M. K.; Wang, L.; Yu, L. *Chem. Mater.* **2000**, *12*, 2988. (b) Wang L.; Ng, M. K.; Yu, L. *Phys. Rev. B* **2000**, *62*, 8, 4973.
(11) Wang, L.; Zhang, Y.; Wada, T.; Sasabe, H. *Appl. Phys. Lett.* **1996**, *69*, 728.
(12) Thelakkat, M.; Schmitz, C.; Hohle, C.; Strohriegl, P.; Schmidt, H. W.; Hofmann, U.; Schloter, S.; Haarer, D. *Phys. Chem. Chem. Phys.* **1999**, *1*, 1693.
(13) Ogino, K.; Park, S. H.; Sato, H. *Appl. Phys. Lett.* **1999**, *74* (26), 3936.
(14) Lundquist, P. M.; Wortmann, R.; Geletneky, C.; Twieg, R. J.; Jurich, M.; Lee, V. Y.; Moylan, C. R.; Burland, D. M. *Science* **1996**, *274*, 1182.

10.1021/cm020702i CCC: $25.00
Published on Web 02/14/2003

Scheme 1. Synthesis Method Involving Ullmann Coupling for the DCTA Charge-Transport Component of the DCST−DCTA Glass

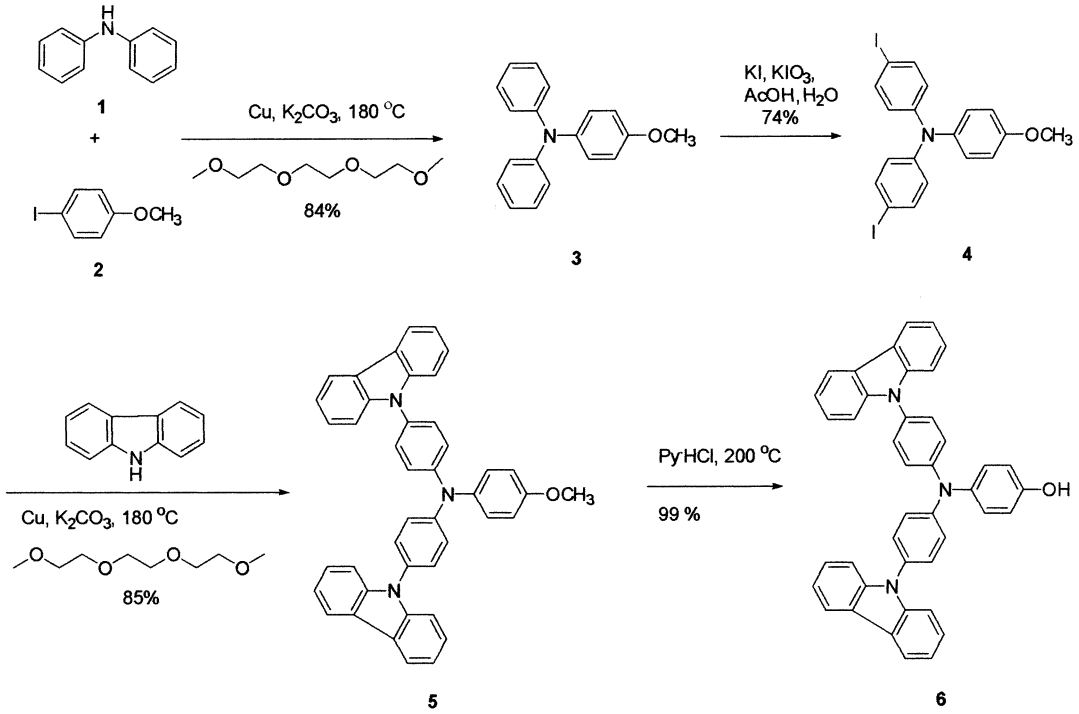

A true monolithic photorefractive composition contains a single component endowed with all the multiple functions. Currently, such true single-component systems are rare and usually at least a sensitizer is added in low concentration to a multifunctional single component. Actually, having the photosensitizer as an independent component can also be seen as an advantage. The spectral sensitivity can be chosen more freely as the magnitude of the absorption can be tuned by the level of doping. As the concentration of the photosensitizer is very low, problems with phase separation are generally not of much concern for this component.

In one such approach, multifunctional materials were described that combined triarylamines, which possess photoconductive properties, and NLO chromophores, which provide electro-optic function, in one molecule.[12,15,16] In this class, the system DR1−DCTA (4,4′-di(carbazol-9-yl)-4″-(2-{*N*-ethyl-*N*-[4-(nitrophenylazo)-phenyl]amine}ethoxy) triphenylamine) has been investigated quite thoroughly. This molecule has a Disperse Red 1 (DR1) type chromophore and a dicarbazole-substituted triarylamine (DCTA) moiety as the hole-transporting component. Because the central bond −N═N− in DR1 is known to show a large photochromic effect through cis−trans isomerization, we wished to identify alternative chromophores without this competing non-photorefractive grating.[17] Furthermore, the DR1−DCTA compounds needed a quite large amount of plasticizer to lower the glass transition temperature down to room temperature. Therefore, we also aimed to lower the glass transition temperature of our new combination of DCTA and chromophore by changing the length of the linker group. The ultimate goal to completely avoid plasticizer and reach a true single-component PR glass with T_g around room temperature is intriguing (the photosensitizer can remain a separate component as discussed above).

We report here the synthesis and physical properties of several related amorphous multifunctional photorefractive materials with the same charge-transport segment but covalently linked with different size spacers to a single aminodicyanostyrene (DCST) chromophore. In the course of the development of this class of materials many different chromophores (such as tolanes and 1-R-1H-pyridine-4-ylidene-ethylidenemalononitrile) were examined in combination with DCTA but the DCST materials discussed here provided the overall best match in terms of stability and photorefractive function. Whereas the DCST−DCTA glasses reported here do not possess the most outstanding photorefractive properties, the general design principles and methods discussed here should be useful in the creation of future photorefractive systems.

Results and Discussion

Synthesis. With the goal of optimizing PR function (gain, speed, and stability) we have synthesized the DCST−DCTA compounds **14a**−**14c**. Simple amine-donor-substituted dicyanostyrene (DCST) chromophores are already well-known as dopants in PVK-based PR composites.[6,18,19] Here, saturated chains with different lengths are employed to covalently link the common charge-transporting triarylamine and birefringent chromophore sections. The synthesis of these new covalently linked materials is presented in Schemes 1 and 2.

(15) Hohle, C.; Hofmann, U.; Schloter, S.; Thelakkat, M.; Strohriegl, P.; Haarer, D.; Zilker, S. J. *J. Mater. Chem.* **1999**, *9*, 2205.
(16) Hofmann, U.; Grasruck, M.; Leopold, A.; Schreiber, A.; Schloter, S.; Hohle, C.; Strohriegl, P. Haarer, D.; Zilker, S. J. *J. Phys. Chem. B* **2000**, *104*, 3887.
(17) Schloter, S.; Schreiber, A.; Grasruck, M.; Leopold, A.; Kol'chenko, M.; Pan, J.; Hohle, C.; Strohriegl, P.; Zilker, S. J.; Haarer, D. *Appl. Phys. B* **1999**, *68*, 899.
(18) Diaz-Garcia, M. A.; Wright, D.; Casperson, J. D.; Smith, B.; Glazer, E.; Moerner, W. E.; Sukhomlinova, L. I.; Twieg, R. J. *Chem. Mater.* **1999**, *11*, 1784.

Scheme 2. Synthesis Scheme for the Complete Multifunctional DCST−DCTA Glass Showing the Preparation of the Chromophore, Linking Unit, and Their Attachment to the Transport Component

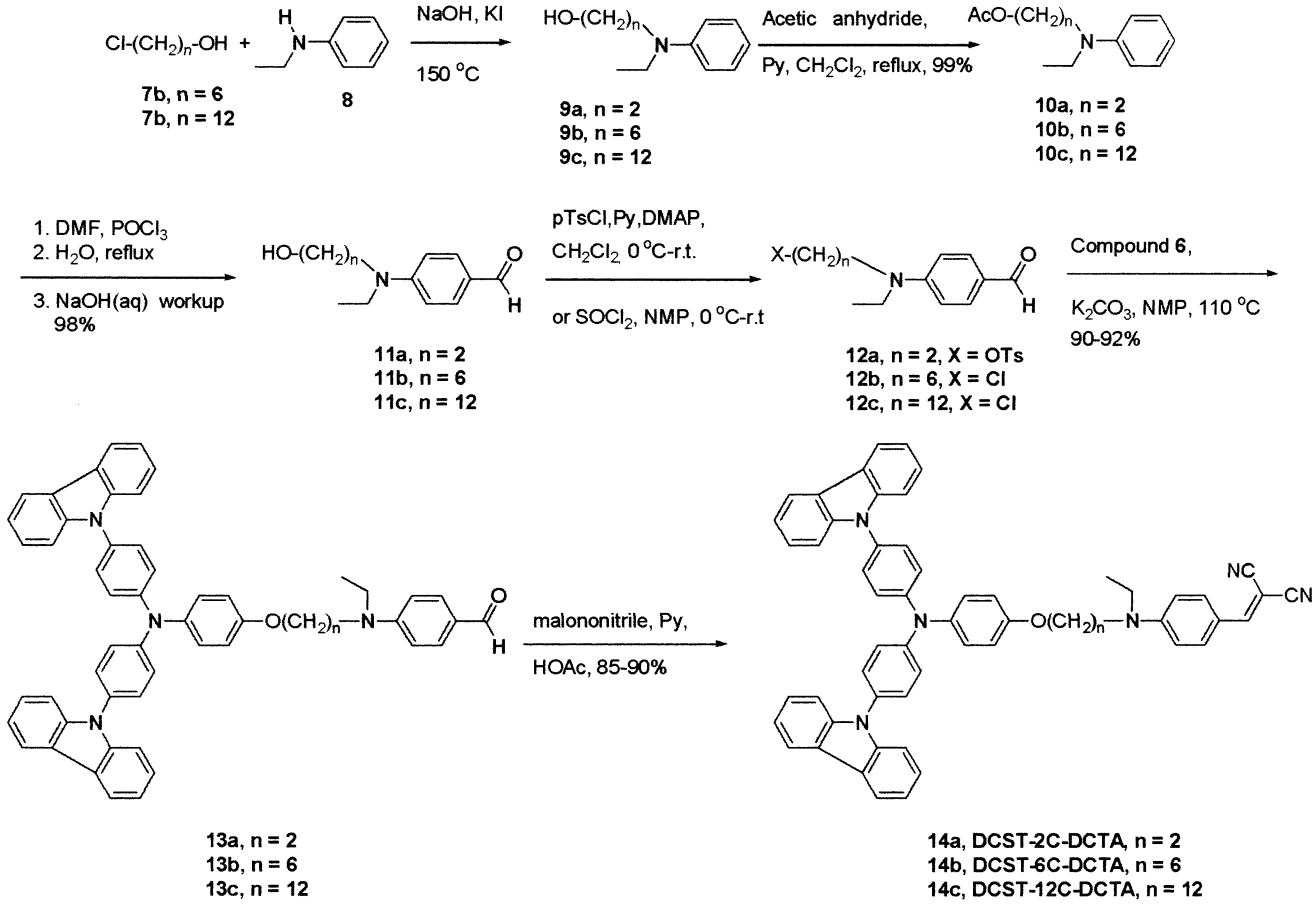

The synthesis of the charge-transfer section **6** (the DCTA part of the molecule) was adapted from the literature[15] with some improvements (Scheme 1). For the two Ullmann coupling procedures involved in the preparation of **3** and **5**, the literature route was modified. For this reaction we substituted triethylene glycol dimethyl ether as solvent instead of the use of a crown ether.[20] A yield of 80−90% was typically obtained despite the high reaction temperatures required in the range of 180−200 °C. The cleavage of the methyl group on **5** was conducted in pyridine hydrochloride at 200 °C to give the phenolic charge-transport precursor **6** in quantitative yield.

As can be seen in Scheme 2, the formation of the linking unit (from **12** to **13**) by the Williamson reaction is completed prior to Knoevenagel condensation in which the aldehyde is converted to the dicyanostyrene. The tosylate-substituted **12a** or chloride-substituted **12b** and **12c** benzaldehyde precursors required for the Williamson reaction were prepared from either commercially available **9a** or easily prepared aniline derivatives **9b** and **9c** by using a Vilsmeier−Haack reaction followed by a tosylation or chlorination reaction. The final Knoevenagel condensation of the benzaldehyde derivative with malononitrile was done in pyridine using acetic acid as a catalyst with easy workup and yields of 85−90%. The DCST−DCTA products **14a**−**14c** were purified by column chromatography followed by dissolution in CH_2Cl_2 and precipitation from methanol.

UV−Vis Absorption Measurements. As expected, the three DCST−DCTA glasses **14a**−**14c** showed almost identical absorption spectra independent of the linking group (Figure 1). The band with λ_{max} at 434 nm is due to charge transfer in the amino donor−dicyanostyrene acceptor chromophore. The other bands at

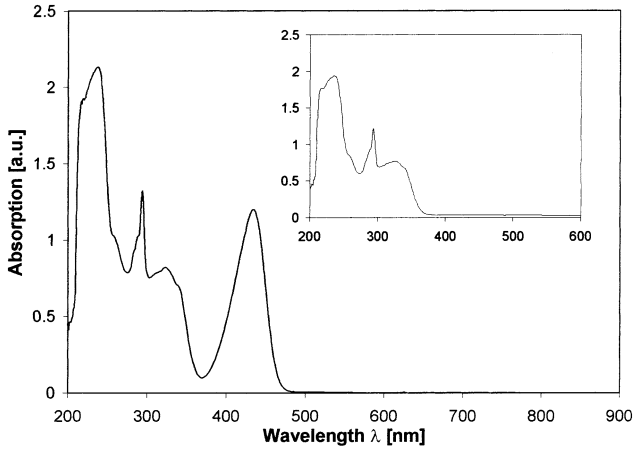

Figure 1. UV−vis absorption spectra of DCST−6C−DCTA in THF. Note the highly symmetrical charge-transfer band centered at about 434 nm due to the dicyanostyrene free of dimer. The inset shows the absorption of the parent charge transport molecule **5** that contains no aminodicyanostyrene.

(19) Grunnet-Jepsen, A.; Wright, D.; Smith, B.; Bratcher, M. S.; DeClue, M. S.; Siegel, J. S.; Moerner, W. E. *Chem. Phys. Lett.* **1998**, *291*, 553.

(20) Miller, R. D.; Lee, V. Y.; Twieg, R. J. *J. Chem. Soc., Chem. Commun.* **1995**, 245.

λ_{max} 238, 294, and 323 nm are due mostly to the triarylamine moiety (see comparison with the inset curve, which is the spectra of the parent charge-transport molecule **5**). No absorption can be observed greater than 490 nm, which allows the use of lasers with $\lambda = 676$ nm for holographic measurements.

It has been demonstrated that many chromophores with large dipole moments tend to aggregate in an antiparallel way to minimize electrostatic energy.[21] As such, some otherwise well-designed chromophores may give unexpectedly low nonlinear optical response due to this dipole−dipole interaction. This has been particularly troublesome in the case of electro-optics where the alignment of chromophores in the electric field is reduced when the dipole−dipole interaction is too strong. A dimer aggregate can usually be observed in the UV−vis absorption measurement as a characteristic concentration-dependent additional peak (or a shoulder) at the lower energy side of the absorption peak.[22,23] In the case of all the DCST−DCTA glasses the absorption around 434 nm appeared as a symmetrical peak and there was no indication of significant dimer formation.

Thermal Properties of DCST−DCTA Glasses. For the creation of useful devices based on organic photorefractive materials, stable and high-quality amorphous glassy materials are required. A combination of differential scanning calorimetry (DSC) and thermal gravimetric analysis (TGA) was used to study the thermochemical stability of the chromophores and to determine the glass transition temperature T_g of the DCST−DCTA materials. All three DCST−DCTA compounds are thermally stable up to about 350−360 °C in a nitrogen atmosphere, as revealed by both TGA and DSC. At 10 °C/min heating the TGA shows a weight loss onset near 360 °C and the DSC shows a large exothermic peak with an onset of about 350 °C. Both of these events are due to some irreversible chemical change involving evolution of small volatile fragments. Only glass transitions were observed for all three DCST−DCTA compounds during first and second heatings (to temperatures well below the decomposition temperature). All DCST−DCTA compounds form stable glasses, that is, no recrystallization occurs upon cooling at 10 °C/min. As the linking group becomes longer (**14a**, $n = 2$; **14b**, $n = 6$; **14c**, $n = 12$) the glass transition temperature T_g gradually drops (Figure 2) as the longer chain gives the two terminal moieties more freedom to rotate or move relative to each other. The modification of the linker group proved to be a viable path to lower the glass transition temperature. The decrease of nearly 50 °C is quite promising and allows reducing the amount of plasticizer for PR composites (from 30 to 20 wt %, see below). With additional modifications it seems feasible to push the T_g even further down and eventually reach an initial T_g at room temperature.

Cyclic Voltammetry Study. Cyclic voltammetry (CV) was employed to investigate the redox behavior of the DCST−DCTA compounds. The anodic scan provides information about ionization processes so that the highest occupied molecular orbital (HOMO) energy can be calculated. The absolute and relative HOMO levels of the components of PR materials play an important role in charge trap dynamics[19] and photogeneration efficiency.[24] In this study, the HOMO values were calculated from the oxidation potential versus the internal standard of ferrocene/ferrocenium (Fc) using the semiempirical method described in the literature[25] and are given as negative values with respect to the zero vacuum energy level. The HOMO value for standard Fc is considered to be −4.8 eV obtained from the calculated value of −4.6 eV for a standard electrode potential for a normal hydrogen electrode (NHE) on the zero vacuum level and the value of 0.2 V for Fc vs NHE.[26] All three glasses **14a**−**14c** have three oxidation waves (Figure 3) corresponding to mono-, di-, and trication radicals. In all cases, at least the first oxidation is reversible and its half oxidation potential was used to calculate the HOMO, which is −5.18 eV. The possible oxidation of the DCST chromophore part of the molecule was buried in the second oxidation wave of the DCTA transport unit. With use of the same method, the HOMO positions of DCST−2C−DCTA and DCST−12C−DCTA were determined to be −5.19 and −5.18 eV, respectively (identical within experimental error).

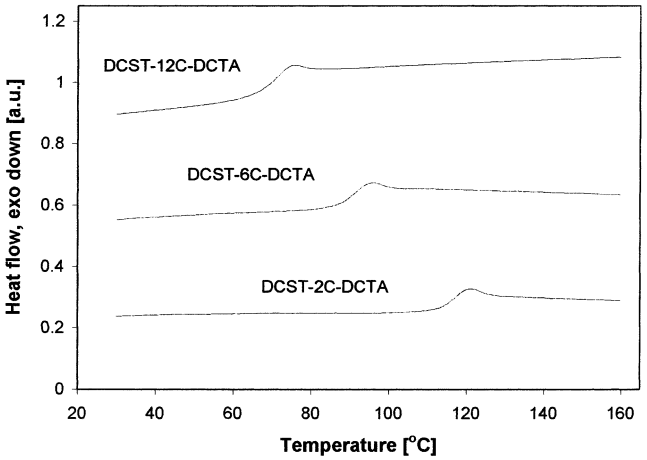

Figure 2. Glass transitions of DCST−DCTA glasses with different length links between the charge transport and nonlinear optical chromophore parts of the molecules. The T_g is obtained from the second heating by DSC. The curves for the different glasses have been vertically offset for better legibility.

Molecular Orientation of Chromophores in PR Composites. To facilitate the reorientation of the chromophores in an electric field, the diisooctyl phthalate plasticizer (DOP) is added to the DCTA−DCSTs to adjust the glass transition temperature T_g down to room temperature. The wt % of plasticizer required to achieve a room-temperature glass was in the range of 20−30 wt % depending on the linker length. Each photorefractive composite was sensitized with 1 wt % of C_{60}, which

(21) Würthner, F.; Yao, S. *Angew.* Chem., Int. Ed. **2000**, *39*, 11, 1978.
(22) Würthner, F.; Yao, S.; Schilling, J.; Wortmann, R.; Redi-Abshiro, M.; Mecher, E.; Gallego-Gomez, F.; Meerholz, K. *J. Am. Chem. Soc.* **2001**, *123*, 2810.
(23) Würthner, F.; Wortmann, R.; Meerholz, K. *ChemPhysChem* **2002**, *3*, 17.
(24) Hendrickx, E.; Kippelen, B.; Thayumanavan, S.; Marder, S. R.; Persoons, A.; Peyghambarian, N. *J. Chem. Phys.* **2000**, *112* (21), 9557.
(25) Pommerehne, J.; Vestweber, H.; Guss, W.; Mahrt, R. F.; Bassler, H.; Porsch, M.; Daub, J. *Adv. Mater.* **1995**, *7*, 551.
(26) Bard, A. J.; Faulkner, L. R. *Electrochemical Methods: Fundamental and Applications*; Wiley: New York, 1980; p 634. Koepp, H. M.; Wendt, H.; Strehlow, H. Z. *Electrochemistry* **1960**, 64.

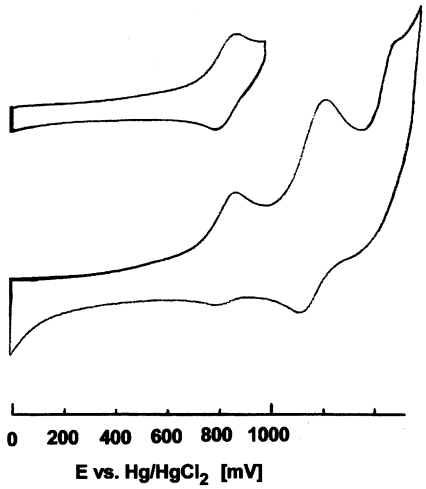

Figure 3. Cyclic voltammograms of DCST−6C−DCST as measured in 0.1 M $TEABF_4$/acetonitrile at a sweep rate of 300 mV/s. The top curve shows only the reversible first oxidation wave.

leads to an absorption α of some tens of inverse centimeters at a wavelength $\lambda = 676$ nm. The actual photorefractive sample is created by dissolving all the components in benzene, freezing the solution in liquid nitrogen, and drying the composite in a vacuum while slowly warming up to room temperature. The solvent-free mixture was melted on an ITO-coated glass substrate and subsequently sandwiched between a second ITO-coated glass substrate. The thickness of the samples are typically around 100 μm, dictated by the Teflon spacers used between the glass substrates.

The field-induced orientation of the molecules is measured in a transient ellipsometry experiment with the sample placed between crossed polarizers and tilted with respect to the light wavevector. The electric field E is applied as a step function in time while the transmitted laser beam is monitored ($\lambda = 905$ nm). The observed change in refractive index Δn is proportional to the squared electric field $\Delta n \propto E^2$, as expected for orientational nonlinearities. Figure 4a shows the induced refractive index change for different amounts of plasticizer DOP in DCST−6C−DCTA. The orientation takes place over several orders of magnitude in time and does not level off in the experimental window. Adding 5% of plasticizer lowers the glass transition temperature about 10 °C and speeds up the orientation about 1 order of magnitude.

Figure 4b shows a comparison of the temporal response examined by transient ellipsometry for the three DCST−DCTAs **14a**−**14c** that have been plasticized to produce roughly the same $T_g \approx 20$ °C. Although one might assume that the orientational behavior might be similar for samples with the same T_g, one observes large differences in the orientation speed of the chromophores. (Here, we assume that the nonlinearity per molecule is approximately the same for all the samples, an approximation that follows from the similar absorption spectra that imply no large charge transfer between the DCTA and the DCST portions of the molecule.) The faster orientation of DCST−12C−DCTA compared to DCST−6C−DCTA and DCST−2C−DCTA should also result in better photorefractive performance.

The orientation of all the glassy DCST−DCTA molecules is, in fact, much slower than that for the standard

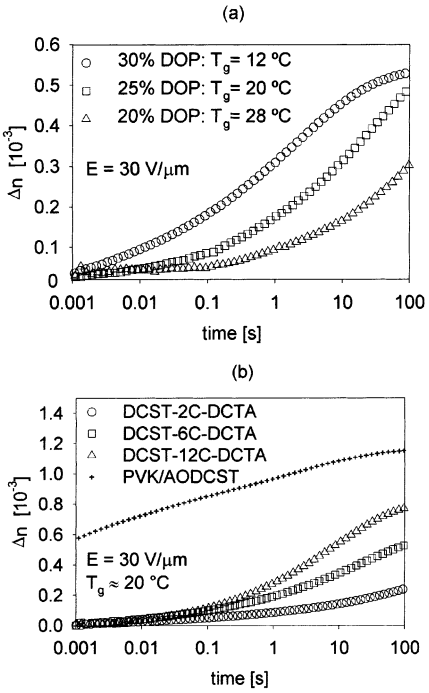

Figure 4. Transient ellipsometry experiments on DCST−DCTA samples: (a) growth of Δn at 30 V/μm for DCST−6C−DCTA with different amounts of DOP plasticizer added, producing samples with different T_g's; (b) growth of Δn at 30 V/μm for the three DCST−nC−DCTAs with different linker lengths plasticized to the same T_g compared with the guest−host system of a DCST derivative (AODCST) in PVK.

composites with PVK as the charge-transport polymer and the DCST derivative AODCST as the chromophore (see Figure 4b). For several such guest−host systems a considerable part of the orientational response already occurs below a millisecond, several orders of magnitude faster than that for the DCST−DCTAs. Considering the large spread of orientation times for the various DCST composites at the same glass transition temperature T_g, one sees that the macroscopic entity T_g is not a fully sufficient measure of the microscopic orientational behavior of the chromophores in an electrical field.

Photorefractive Characterization: Two-Wave Mixing. The two-wave mixing measurements are conducted at the wavelength $\lambda = 676$ nm in a standard setup.[3] The two beams have an intensity ratio of 1:1 and are adjusted to a total writing intensity of $I = 1$ W/cm^2 at the peak.

The time traces of the beam coupling (Figure 5a for DCST−6C−DCTA) show two clearly distinguishable time constants: a fast one around some tens of milliseconds and a slow one on the time scale of several seconds. The slow time constant corresponds well with the transient ellipsometry measurements and leads to the conclusion that in this system the main part of the photorefractive response is limited by the reorientation of the chromophore.

The gain coefficients Γ of the energy transfer between the two beams are shown as a function of the applied external field in Figure 5b. The photorefractive beam coupling is seen to increase the most with the longer linkers. Whereas the gain coefficients for DCST−6C−DCTA are only slightly larger as compared with those of DCST−2C−DCTA, the increase for the long linker compound DCST−12C−DCTA is larger, about a factor

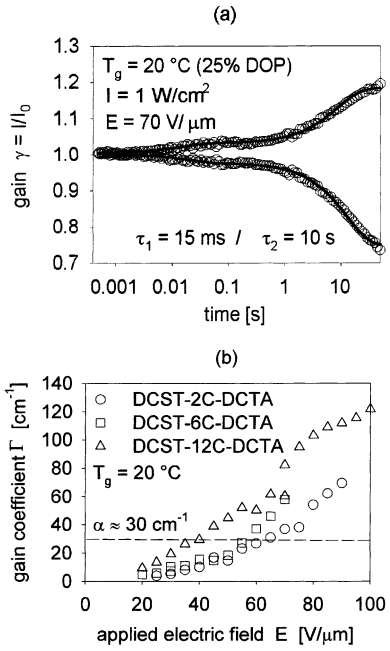

Figure 5. Two-wave mixing for DCST−DCTA samples with the glass transition temperature adjusted near room temperature: (a) the buildup of the beam coupling for DCST−6C−DCTA shows two time constants; (b) gain coefficient Γ as a function of the applied electric field E for DCST−nC−DCTA with the three linker lengths.

of 2. Net gain ($\Gamma > \alpha$) is achieved for moderate field strengths between 40 and 55 V/μm.

The general trend of the photorefractive measurements corresponds well with the data obtained by transient ellipsometry. The longer linker between the charge-transport part and the nonlinear optical moiety seems to be beneficial, but a more detailed understanding of this effect in terms of the microscopic ability to reorient and to produce a larger steady-state gain coefficient will require further study. The overall PR performance of these DCST−DCTA organic glasses is not enhanced compared to that of earlier systems with PVK as the charge-transport polymer with the same DCST chromophore. However, the improvements of the PR response achieved by the simple change of the linker length shows some potential for further improvements.

Comparison with DR1−DCTA. The comparison of our DCST−DCTA compounds with the published work on DR1−DCTA is of special interest and allows further conclusions for the optimal design of this type of organic glasses. The glass transition temperature of DR1−DCTA is around 120 °C,[15] which compares fairly well with our shortest linker DCST−2C−DCTA compound. With the longer linker approach, we also improved the T_g with respect to DR1−DCTA. Looking at the amount of plasticizer necessary, the DR1−DCTA required 28 wt % of DOP to lower the Tg down to 21 °C,[15] which again compares well with our DCST−2C−DCTA molecule. For the two longer linker compounds, we clearly gain an advantage by requiring only 25 and 20 wt %, respectively.

The absorption band of the DCST−DCTA system is blue-shifted about 30 nm compared to that of DR1−DCTA (465 nm in dioxane).[15] The transparency window for photorefractive operation in DCST−DCTA is therefore considerably larger in the visible part of the spectrum. Only limited ellipsometry data is published for DR1−DCTA.[16] The molecular orientation is very dispersive, similar to the DCST−DCTAs, happening over many orders of magnitude in time. The time traces for both compounds look qualitatively the same.

The photorefractive gain coefficients for DR1−DCTA reach $\Gamma = 90$ cm^{-1} at an applied field of $E = 80$ V/μm.[12,15] This gain coefficient is considerably larger than that for the two shorter linker DCST−DCTAs and slightly less than that for the long linker DCST−12C−DCTA. Looking at the speed of two-wave mixing, DR1−DCTA shows a first response time of 30−40 ms at 80 V/μm [12,15] that compares well with our first time constant of 15 ms at comparable electric fields and light intensities. As the photorefractive speed depends on many factors (e.g., the experimental conditions and the exact fitting procedure), this kind of comparison has to be interpreted with some care. However, we can safely conclude that the DR1−DCTA and DCST−DCTA compounds show the same order of magnitude in photorefractive speed.

All things considered, we have obtained comparable results for the DCST−DCTA systems as for the earlier published work on DR1−DCTA. By modifying the linker group, we obtain an advantage in the lower amount of plasticizer required and slightly improved photorefractive performance. The main disadvantage of DR1 compared to our DCST compounds remains the photochromic grating occurring in DR1 by the cis−trans isomerization of the azo group. The absence of such a photochromic effect in DCST chromophores ensures a purely photorefractive effect and more potential for practical developments.

Conclusions

We have combined the functions of optical nonlinearity, birefringence, and charge transport into a single molecule by attaching an NLO chromophore to a charge-transport moiety to produce a glassy morphology. The longer linking group not only lowers the glass transition temperature T_g but also influences the photorefractive performance of the samples. Although the T_g of all samples was held constant at ambient temperature by adjustment with plasticizer addition, the longer linker glasses show significantly faster molecular reorientation in an electrical field. The photorefractive gain coefficient is larger for longer linkers with about a 2-fold increase going from the 2-carbon atom linker to 12. Introducing further modification to the linker group and addition of inert spacer groups seems to be an open pathway to decrease the T_g further down to room temperature and in parallel boost the PR properties as well.

The gain coefficient and the photorefractive response time of these multifunctional systems are, so far, clearly inferior to the dicyanostyrene chromophores as simple dopants in a PVK matrix.[6,18] In the DCST−DCTA compounds the photorefractive speed seems to be limited by the molecular orientation. This outcome is in clear contrast to the speed limits occurring due to charge redistribution in the PVK systems. The reasons for this significantly different behavior is not yet clear and will be the subject of further research.

Experimental Section

NMR spectra were measured with a Bruker AMX 300, UV−vis spectra with a HP 8453 spectrophotometer, melting points

with Olympus BH-2 polarized light microscope equipped with a Mettler FP5 temperature controller and FP52 hot stage, thermal analysis (glass transition temperature and decomposition temperature) with TA Instruments DSC 2920 and TA Instruments TGA 2950.

Cyclic voltammetry was conducted using a three-electrode cell equipped with an IBM EC 225[1A] voltammetric analyzer and a HP 7046B X-Y recorder. Electrodes are a platinum disk working electrode, platinum wire counter electrode, and Hg/$HgCl_2$/NaCl reference electrode. Samples were prepared in degassed acetonitrile (freshly distilled from CaH_2) solutions containing 0.1 M tetraethylammonium tetrafluroborate as the supporting electrolyte.

(4-Methoxyphenyl)diphenylamine (3). A mixture of diphenylamine (15 g, 88.6 mmol), 4-iodoanisole (24.9 g, 106 mmol), copper powder (5.67 g, 89 mmol), potassium carbonate (29.4 g, 213 mmol), and triethyleneglycol dimethyl ether (20 mL) was mechanically stirred under the protection of dry nitrogen at 200 °C for 26.5 h. The reaction mixture was cooled, diluted with ethyl acetate, and filtered through a short pad of silica gel. The filtrate was concentrated and refrigerated. The resulting white crystalline product was collected by vacuum filtration and washed with petroleum ether (20.6 g, 84%): mp 104 °C (lit[27] 103−105 °C). ^{1}H NMR (300 MHz, $CDCl_3$): δ 3.82 (s, 3 H), 6.87 (d, J = 8.90 Hz, 2 H), 6.97 (t, J = 7.11 Hz, 2 H), 7.09 (m, 6 H), 7.24 (m, 4 H). ^{13}C NMR (75 MHz, $CDCl_3$): δ 55.65, 114.94, 122.02, 123.06, 127.49, 129.25, 140.96, 148.36, 156.33.

4,4′-Diiodo-4″-methoxytriphenylamine (4). To a stirred mixture of (4-methoxyphenyl)diphenylamine (**3**) (10 g, 36.4 mmol), potassium iodide (7.8 g, 47 mmol), acetic acid (150 mL), and water (15 mL) at 80 °C was added potassium iodate in one portion (7.78 g, 36.4 mmol) and the resulting mixture was stirred and heated for 3.5 h. After the reaction, most of the acetic acid was removed by rotary evaporation. The black residue was dissolved in ethyl acetate and washed several times with water and sodium bicarbonate solution. The organic layer was dried over magnesium sulfate, filtered, and concentrated, and the crude material was purified by column chromatography (eluent: EtOAc/hexane = 1/9) to give the product as a clear glass (14.3 g, 74%), no mp. ^{1}H NMR (300 MHz, $CDCl_3$): δ 3.80 (s, 3 H), 6.78 (d, J = 8.94 Hz, 4 H), 6.84 (d, J = 9.01 Hz, 2 H), 7.03 (d, J = 9.01 Hz, 2 H), 7.48 (d, J = 8.86 Hz, 4 H). ^{13}C NMR (75 MHz, $CDCl_3$): δ 55.66, 84.91, 115.20, 124.82, 127.72, 138.25, 139.64, 147.53, 156.98.

4,4′-Di(carbazol-9-yl)-4″-methoxytriphenylamine (5). A mixture of 4,4′-diiodo-4″-methoxytriphenylamine (**4**) (13 g, 25 mmol), carbazole (10.3 g, 62 mmol), copper powder (3.16 g, 50 mmol), potassium carbonate (13.6 g, 99 mmol), and triethyleneglycol dimethyl ether (25 mL) was mechanically stirred for 24 h under the protection of dry nitrogen at 200 °C. After cooling, the mixture was precipitated in methanol and the resulting solid was purified by column chromatography (eluent: toluene) to give the product as a white solid (13.7 g, 85%): glass, no mp. ^{1}H NMR (300 MHz, $CDCl_3$): δ 3.89 (s, 3 H), 7.02 (d, J = 8.79 Hz, 2 H), 7.31−7.54 (m, 22 H), 8.20 (d, J = 7.69 Hz, 4 H). ^{13}C NMR (75 MHz, $CDCl_3$): δ 55.74, 110.05, 115.44, 120.00, 120.53, 123.45, 123.73, 126.09, 128.17, 128.34, 131.61, 140.17, 141.30, 147.23, 157.22.

4,4′-Di(carbazol-9-yl)-4″-hydroxytriphenylamine (6). A mixture of 4,4′-di(carbazol-9-yl)-4″-methoxytriphenylamine (**5**) (7.44 g, 12.3 mmol) and pyridine hydrochloride (40 g) was stirred at 200 °C for 6 h under the protection of dry nitrogen. After cooling, the reaction mixture was poured into cold water and the white solid precipitate was collected by vacuum filtration (7.2 g, 99%): glass, no mp. ^{1}H NMR (300 MHz, $CDCl_3$): δ 4.75 (s, br, 1 H), 6.90 (s, br, 2 H), 7.25−7.45 (m, 22 H), 8.15 (d, J = 7.5 Hz, 4 H). ^{13}C NMR (75 MHz, $CDCl_3$): δ 110.05, 116.94, 120.05, 120.54, 123.45, 123.75, 126.14, 128.56, 128.77, 131.74, 140.65, 141.34, 147.25, 153.24.

6-(*N*-Ethylanilino)hexanol (9b). A mixture of *N*-ethylaniline (16.1 g, 133 mmol), 6-chloro-1-hexanol (20 g, 146 mmol), sodium hydroxide (6.4 g, 160 mmol), and potassium iodide (0.044 g, 0.3 mmol) was stirred at 150 °C for 12 h. The reaction mixture was Kugelrohr-distilled and the product was collected as a clear liquid (12 g, 41%). ^{1}H NMR (300 MHz, $CDCl_3$): δ 1.17 (t, J = 7.04 Hz, 3 H), 1.40 (m, 4 H), 1.59 (m, 4 H), 3.27 (t, J = 7.68 Hz, 2 H), 3.37 (q, J = 7.04 Hz, 2 H), 3.64 (t, J = 6.57 Hz, 2 H), 6.68 (m, 3 H), 7.23 (m, 2 H). ^{13}C NMR (75 MHz, $CDCl_3$): δ 12.47, 25.89, 27.21, 27.70, 32.92, 45.10, 50.53, 62.97, 112.03, 115.50, 129.41, 148.16.

12-(*N*-Ethylanilino)dodecanol (9c). A mixture of *N*-ethylaniline (5.35 g, 44.1 mmol), 12-bromo-1-dodecanol (3.9 g, 14.7 mmol), sodium hydroxide (0.71 g, 17.6 mmol), and a trace of potassium iodide was stirred at 150 °C for 4 h. After cooling, the reaction mixture was diluted with ethyl acetate, washed with water several times, dried over magnesium sulfate, and concentrated. The resulting oil was purified by column chromatography (solvent: EtOAc/hexane = 1/9) to give the product as a clear liquid (4.48 g, 99.8%). ^{1}H NMR (300 MHz, $CDCl_3$): δ 1.14 (t, J = 7.2 Hz, 3 H), 1.29 (m, 16 H), 1.57 (m, 4 H), 3.23 (t, J = 7.5 Hz, 2 H), 3.35 (q, J = 7.2 Hz, 2 H), 3.64 (t, J = 6.6 Hz, 2 H), 6.60−6.67 (m, 3 H), 7.18−7.26 (m, 2 H). ^{13}C NMR (75 MHz, $CDCl_3$): δ 12.45, 25.88, 27.37, 27.69, 29.56 (m), 29.69 (m), 32.97, 45.04, 50.61, 63.20, 112.04, 115.43, 129.33, 148.16.

2-(*N*-Ethylanilino)ethyl Acetate (10a). A mixture of 2-(*N*-ethylanilino)ethanol (**9a**) (20 g, 121 mmol), acetic anhydride (17.1 mL, 181 mmol), pyridine (29.4 mL, 364 mmol), and dichloromethane (160 mL) was refluxed for 24 h. After cooling, the white precipitate was filtered off with a short pad of silica gel and the organic solution was washed with water, dried over magnesium sulfate, concentrated, and dried in the vacuum oven to give the product as a clear liquid (24.1 g, 96%). ^{1}H NMR (300 MHz, $CDCl_3$): δ 1.18 (t, J = 7.05 Hz, 3 H), 2.06 (s, 3 H), 3.41 (q, J = 7.06 Hz, 2 H), 3.56 (t, J = 6.47 Hz, 2 H), 4.24 (t, J = 6.47 Hz, 2 H), 6.67−6.75 (m, 3 H), 7.23 (m, 2 H). ^{13}C NMR (75 MHz, $CDCl_3$): δ 12.40, 21.07, 45.39, 48.98, 61.89, 112.13, 116.38, 129.52, 147.76, 171.16.

6-(*N*-Ethylanilino)hexyl Acetate (10b). A mixture of 6-(*N*-ethylanilino)hexanol (**9b**) (12 g, 54.2 mmol), acetic anhydride (7.67 mL, 81.3 mmol), pyridine (13.2 mL, 163 mmol), and dichloromethane (96 mL) was refluxed for 24 h. After cooling, the white precipitate was filtered through a short pad of silica gel and the organic solution was washed with water, dried over magnesium sulfate, concentrated, and dried in the vacuum oven to give the product as a clear liquid (14.1 g, 99%). ^{1}H NMR (300 MHz, $CDCl_3$): δ 1.15 (t, J = 7.04 Hz, 3 H), 1.38 (m, 4 H), 1.61 (m, 4 H), 2.05 (s, 3 H), 3.25 (t, J = 7.58 Hz, 2 H), 3.36 (q, J = 7.04 Hz, 2 H), 4.07 (t, J = 6.68 Hz, 2 H), 6.65 (m, 3 H), 7.21 (m, 2 H). ^{13}C NMR (75 MHz, $CDCl_3$): δ 12.46, 21.16, 26.06, 27.02, 27.62, 28.79, 45.11, 50.47, 64.63, 111.98, 115.50, 129.40, 148.11, 171.36.

12-(*N*-Ethylanilino)dodecyl Acetate (10c). A mixture of 12-(*N*-ethylanilino)dodecanol (**9c**) (4.5 g, 14.7 mmol), acetic anhydride (2.1 mL, 22.1 mmol), pyridine (3.57 mL, 44.2 mmol), and dichloromethane (50 mL) was refluxed for 24 h. After cooling, the white precipitate was filtered off and the organic solution was washed with water, dried over magnesium sulfate, and concentrated. The oil obtained was purified by column chromatography (solvent: EtOAc/hexane = 1/9) to give the product as a clear liquid (5.0 g, 98%). ^{1}H NMR (300 MHz, $CDCl_3$): δ 1.16 (t, J = 7.2 Hz, 3 H), 1.30 (m, 16 H), 1.61 (m, 4 H), 2.06 (s, 3 H), 3.25 (t, J = 7.8 Hz, 2 H), 3.37 (q, J = 7.2 Hz, 2 H), 4.07 (t, J = 6.9 Hz, 2 H), 6.61−6.69 (m, 3 H), 7.19−7.27 (m, 2 H). ^{13}C NMR (75 MHz, $CDCl_3$): δ 12.47, 21.16, 26.08, 27.38, 27.71, 28.79, 29.40, 29.71 (m), 29.79 (m), 45.05, 50.62, 64.75, 112.04, 115.45, 129.34, 148.24, 171.20.

4-[*N*-Ethyl-*N*-(2-hydroxyethyl)amino]benzaldehyde (11a). Phosphorus oxychloride (11.9 mL, 128 mmol) was added dropwise to stirred dry DMF (32 mL, 413 mmol) at 0 °C. The red mixture was kept stirring at this temperature for 30 min and then 2-(*N*-ethylanilino)ethyl acetate (**10a**) (24.1 g, 116 mmol) was added to the mixture at 0 °C. The resulting green solution was then heated at 90 °C for 2 h. After this time the mixture was cooled to room temperature and water (100 mL) was slowly added to the mixture, which began to boil due to the exothermic reaction. The boiling was maintained for 10

(27) Gauthier, S.; Frèchet, J. M. M. *Synthesis* **1987**, 383.

min, and then after the mixture was again cooled to room temperature, the excess acid in the mixture was neutralized by careful addition of aqueous sodium hydroxide. The resulting mixture was extracted with ethyl acetate and the organic layer was washed with water, dried over magnesium sulfate, concentrated, and flash chromatographed to give a yellow oil (22.2 g, 99%), which crystallized upon standing in a refrigerator: mp 45 °C. ^{1}H NMR (300 MHz, $CDCl_3$): δ 1.20 (t, J = 7.15 Hz, 3 H), 2.58 (s, br, 1 H), 3.48 (q, J = 7.10 Hz, 2 H), 3.55 (t, J = 6.01 Hz, 2 H), 3.83 (t, J = 6.00 Hz, 2 H), 6.71 (d, J = 8.90 Hz, 2 H), 7.65 (d, J = 8.63 Hz, 2 H), 9.64 (s, 1 H). ^{13}C NMR (75 MHz, $CDCl_3$): δ 12.07, 45.89, 52.38, 60.06, 111.17, 125.10, 132.45, 152.98, 190.41.

This procedure was also used for the synthesis of **11b** and **11c**.

4-[*N*-Ethyl-*N*-(6-hydroxyhexyl)amino]benzaldehyde (11b). With use of the procedure above and starting with phosphorus oxychloride (5.5 mL, 59 mmol), dry DMF (14.5 mL, 187 mmol), and 6-(*N*-ethylanilino)hexyl acetate (**10b**) (14.1 g, 53.5 mmol), the product was obtained as a yellow oil (13.1 g, 98%). ^{1}H NMR (300 MHz, $CDCl_3$): δ 1.19 (t, J = 7.09 Hz, 3 H), 1.39 (m, 4 H), 1.60 (m, 4 H), 3.32 (t, J = 7.78 Hz, 2 H), 3.42 (q, J = 7.09 Hz, 2 H), 3.64 (t, J = 6.46 Hz, 2 H), 6.64 (d, J = 8.99 Hz, 2 H), 7.69 (d, J = 8.99 Hz, 2 H), 9.67 (s, 1 H). ^{13}C NMR (75 MHz, $CDCl_3$): δ 12.38, 25.80, 27.01, 27.53, 32.81, 45.36, 50.57, 62.85, 110.79, 124.70, 132.44, 152.60, 190.18.

4-[*N*-Ethyl-*N*-(12-hydroxydodecyl)amino]benzaldehyde (11c). With use of the procedure above and starting with phosphorus oxychloride (1.48 mL, 15.8 mmol), dry DMF (3.9 mL, 50.4 mmol), and 12-(*N*-ethylanilino)dodecyl acetate (**10c**) (5.0 g, 14.4 mmol), the product was obtained as a yellow oil (4.4 g, 92%). ^{1}H NMR (300 MHz, $CDCl_3$): δ 1.15 (t, J = 7.2 Hz, 3 H), 1.24 (m, 16 H), 1.53 (m, 4 H), 3.28 (t, J = 7.8 Hz, 2 H), 3.39 (q, J = 7.2 Hz, 2 H), 3.58 (t, J = 6.6 Hz, 2 H), 6.61 (d, J = 9 Hz, 2 H), 7.65 (d, J = 9.0 Hz, 2 H), 9.64 (s, 1 H). ^{13}C NMR (75 MHz, $CDCl_3$): δ 12.35, 25.90, 27.15, 27.49, 29.55 (m), 29.65 (m), 32.92, 45.30, 50.63, 62.99, 110.78, 124.70, 132.37, 152.61, 190.02.

4-[*N*-Ethyl-*N*-(2-tosyloxyethyl)amino]benzaldehyde (12a). A mixture of 4-[*N*-ethyl-*N*-(2-hydroxyethyl)amino]benzaldehyde (**11a**) (1.22 g, 6.3 mmol), tosyl chloride (1.8 g, 9.4 mmol), pyridine (1.5 mL, 18.5 mmol), 4-(dimethylamino)-pyridine (0.077 g, 0.63 mmol), and dichloromethane (20 mL) was stirred at 0 °C for 10 h. The reaction mixture was diluted with dichloromethane, washed with water, dried over magnesium sulfate, and chromatographed on silica gel (eluent: ethyl acetate/hexane = 3/7) to give the product as a yellow oil (1.6 g, 73%). ^{1}H NMR (300 MHz, $CDCl_3$): δ (1.14, J = 7.13 Hz, 3 H), 2.38 (s, 3 H), 3.38 (q, J = 7.10 Hz, 2 H), 3.65 (t, J = 6.02 Hz, 2 H), 4.17 (t, J = 6.01 Hz, 2 H), 6.56 (d, J = 8.93 Hz, 2 H), 7.24 (d, J = 8.03 Hz, 2 H), 7.65 (d, J = 8.96 Hz, 2 H), 7.69 (d, J = 8.20 Hz, 2 H), 9.71 (s, 1 H). ^{13}C NMR (75 MHz, $CDCl_3$): δ 12.15, 21.79, 45.98, 49.01, 66.54, 111.08, 125.81, 127.97, 130.02, 132.25, 132.60, 145.31, 151.81, 190.23.

4-[*N*-Ethyl-*N*-(6-chlorohexyl)amino]benzaldehyde (12b). Thionyl chloride (1.7 mL, 22.9 mmol) was added slowly to a stirred mixture of 4-[*N*-ethyl-*N*-(6-hydroxyhexyl)amino]benzaldehyde (**11b**) (3.8 g, 15.2 mmol) in dry NMP (15 mL) at 0 °C. The reaction was kept at this temperature for 10 min and then at room temperature for half an hour. Saturated sodium bicarbonate water solution was added and the mixture was extracted with ethyl acetate. The organic layer was dried over magnesium sulfate, concentrated, and chromatographed (eluent: ethyl acetate/hexane = 1/9) to give the product as a yellow liquid (3.2 g, 78%), which turned green upon standing in the air. ^{1}H NMR (300 MHz, $CDCl_3$): δ 1.20 (t, J = 7.18 Hz, 3 H), 1.37 (m, 2 H), 1.56 (m, 2 H), 1.64 (m, 2 H), 1.79 (m, 2 H), 3.34 (t, J = 7.88 Hz, 2 H), 3.43 (q, J = 7.18 Hz, 2 H), 3.54 (t, J = 6.58 Hz, 2 H), 6.65 (d, J = 8.96 Hz, 2 H), 7.69 (d, J = 8.96 Hz, 2 H), 9.70 (s, 1 H). ^{13}C NMR (75 MHz, $CDCl_3$): δ 12.38, 26.50, 26.84, 27.43, 32.63, 45.06, 45.38, 50.49, 110.79, 124.85, 132.40, 152.51, 190.10.

This procedure was also used for the synthesis of **12c**.

4-[*N*-Ethyl-*N*-(12-chlorododecyl)amino]benzaldehyde (12c). With use of the procedure above and starting with 4-[*N*-ethyl-*N*-(12-hydroxydodecyl)amino]benzaldehyde (**11c**) (4.34 g, 13 mmol), dry NMP (15 mL), and thionyl chloride (1.42 mL, 20 mmol), the product was obtained as a clear liquid (3.4 g, 74%). ^{1}H NMR (300 MHz, $CDCl_3$): δ 1.18 (t, J = 7.2 Hz, 3 H), 1.26 (m, 16 H), 1.60 (m, 2 H), 1.74 (m, 2 H), 3.30 (t, J = 7.8 Hz, 2 H), 3.42 (q, J = 7.2 Hz, 2 H), 3.50 (t, J = 6.75 Hz, 2 H), 6.63 (d, J = 9.0 Hz, 2 H), 7.69 (d, J = 9.0 Hz, 2 H), 9.67 (s, 1 H). ^{13}C NMR (75 MHz, $CDCl_3$): δ 12.35, 26.99, 27.18, 27.52, 28.98, 29.55 (m), 29.67 (m), 32.77, 45.20, 45.30, 50.64, 110.77, 124.77, 132.30, 152.57, 189.91.

4,4′-Di(carbazol-9-yl)-4″-{2-[*N*-ethyl-*N*-(4-formylphenyl)-amino]}ethoxytriphenylamine (13a). A mixture of 4-[*N*-ethyl-*N*-(2-tosyloxyethyl)amino]benzaldehyde (**12a**) (0.59 g, 1.7 mmol), 4,4′-di(carbazol-9-yl)-4″-hydroxytriphenylamine (**6**) (1 g, 1.7 mmol), potassium carbonate (0.93 g, 6.7 mmol), and NMP (20 mL) was stirred at 110 °C for 4 h. The reaction mixture was then poured into water (300 mL) and the precipitated white solid was collected by vacuum filtration (1.17 g, 90%). ^{1}H NMR (300 MHz, $CDCl_3$): δ 1.30 (t, J = 7.08 Hz, 3 H), 3.62 (q, J = 7.08 Hz, 2 H), 3.87 (t, J = 5.75 Hz, 2 H), 4.21 (t, J = 5.72 Hz, 2 H), 6.78 (d, J = 8.66 Hz, 2 H), 6.96 (d, J = 8.91 Hz, 2 H), 7.26−7.47 (m, 22 H), 7.75 (d, J = 8.97 Hz, 2 H), 8.15 (d, J = 7.66 Hz, 4 H), 9.75 (s, 1 H). ^{13}C NMR (75 MHz, $CDCl_3$): δ 12.36, 46.27, 49.95, 65.78, 109.98, 111.15, 115.91, 119.99, 120.50, 123.42, 123.80, 125.55, 126.06, 128.18 (2 carbons), 131.74, 132.45, 140.70, 141.24, 147.10, 152.45, 155.96, 190.31.

This procedure was also used to synthesize **13b** and **13c**.

4,4′-Di(carbazol-9-yl)-4″-{6-[*N*-ethyl-*N*-(4-formylphenyl)-amino]}hexyloxytriphenylamine (13b). With use of the procedure above and starting with 4-[*N*-ethyl-*N*-(6-chlorohexyl)amino]benzaldehyde (**12b**) (0.40 g, 1.49 mmol), 4,4′-di-(carbazol-9-yl)-4″-hydroxytriphenylamine (**6**) (0.88 g, 1.49 mmol), potassium carbonate (0.82 g, 5.9 mmol), and NMP (20 mL), the product was obtained as a white solid (1.12 g, 92%). ^{1}H NMR (300 MHz, $CDCl_3$): δ 1.21 (t, J = 7.05 Hz, 3 H), 1.42−1.88 (m, 8 H), 3.32−3.55 (m, 4 H), 4.02 (t, J = 5.63 Hz, 2 H), 6.68 (d, J = 8.93 Hz, 2 H), 6.99 (d, J = 8.88 Hz, 2 H), 7.27−7.50 (m, 22 H), 7.72 (d, J = 8.90 Hz, 2 H), 8.16 (d, J = 7.65 Hz, 4 H), 9.70 (s, 1 H). ^{13}C NMR (75 MHz, $CDCl_3$): δ 12.43, 26.24, 27.05, 27.56, 29.51, 45.41, 50.59, 68.23, 110.01, 110.84, 115.92, 119.97, 120.48, 123.41, 123.69, 124.79, 126.05, 128.13, 128.32, 131.58, 132.50, 140.06, 141.26, 147.21, 152.61, 156.67, 190.26.

4,4′-Di(carbazol-9-yl)-4″-{12-[*N*-ethyl-*N*-(4-formylphenyl)amino]}dodecyloxytriphenylamine (13c). With use of the procedure above and starting with 4-[*N*-ethyl-*N*-(12-chlorododecyl)amino]benzaldehyde (**12c**) (1.93 g, 5.5 mmol), 4,4′-di(carbazol-9-yl)-4″-hydroxytriphenylamine (**6**) (3.39 g, 5.7 mmol), potassium carbonate (2.37 g, 17.2 mmol), and NMP (30 mL), the product was obtained as a white solid (4.5 g, 90%). ^{1}H NMR (300 MHz, $CDCl_3$): δ 1.23 (t, J = 7.10 Hz, 3 H), 1.37 (m, 14 H), 1.55 (m, 2 H), 1.66 (m, 2 H), 1.87 (m, 2 H), 3.35 (t, J = 7.65 Hz, 2 H), 3.45 (q, J = 7.10 Hz, 2 H), 4.04 (t, J = 6.45 Hz, 2 H), 6.68 (d, J = 8.70 Hz, 2 H), 7.02 (d, J = 8.70 Hz, 2 H), 7.32−7.54 (m, 22 H), 7.75 (d, J = 8.70 Hz, 2 H), 8.20 (d, J = 7.80 Hz, 4 H), 9.74 (s, 1 H). ^{13}C NMR (75 MHz, $CDCl_3$): δ 12.45, 26.33, 27.27, 27.61, 29.59, 29.65 (m), 29.79 (m), 45.37, 50.71, 68.58, 110.05, 110.90, 116.05, 120.01, 120.49, 123.50, 123.71, 124.88, 126.08, 128.17, 128.34, 131.67, 132.46, 139.99, 141.37, 147.30, 152.70, 156.92, 190.

4,4′-Di(carbazol-9-yl)-4″-(2-{*N*-ethyl-*N*-[4-(2,2-dicyanovinyl)phenyl]amino}ethoxy)triphenylamine, DCST−2C−DCTA (14a). A mixture of **13a** (1.15 g, 1.5 mmol), malononitrile (0.12 g, 1.82 mmol), acetic acid (0.06 g), and pyridine (25 mL) was stirred at room temperature for 4 h. The reaction mixture was then poured into a large quantity of water and the precipitate was collected. Flash chromatography on silica gel was used (eluent: dichloromethane) to purify the product and the solid obtained was further purified by dissolution in CH_2Cl_2 and precipitation from methanol to give the product as a yellow solid (1.06 g, 86%). ^{1}H NMR (300 MHz, $CDCl_3$): δ 1.32 (t, J = 6.98 Hz, 3 H), 3.65 (q, J = 6.99 Hz, 2 H), 3.88 (t, J = 5.22 Hz, 2 H), 4.20 (t, J = 5.29 Hz, 2 H), 6.78 (d, J = 9.08 Hz, 2 H), 6.96 (d, J = 8.87 Hz, 2 H), 7.26−7.51 (m, 23 H), 7.82 (d, J = 8.99 Hz, 2 H), 8.18 (d, J = 7.67 Hz, 4 H). ^{13}C NMR (75

MHz, $CDCl_3$): δ 12.39, 46.48, 50.02, 65.78, 110.00, 111.92, 115.05, 115.90, 116.08, 119.70, 120.04, 120.53, 123.45, 123.87, 126.10, 128.19 (2 carbons), 131.80, 134.18, 140.88, 141.24, 147.08, 152.70, 155.76, 158.10.

This procedure was also used for the synthesis of **14b** and **14c**.

4,4′-Di(carbazol-9-yl)-4″-(6-{*N*-ethyl-*N*-[4-(2,2-dicyanovinyl)phenyl]amino}hexyloxy)triphenylamine, DCST−6C−DCTA (14b). With use of the procedure above and starting with **13b** (1.10 g, 1.34 mmol), malononitrile (0.11 g, 1.67 mmol), acetic acid (0.08 g), and pyridine (20 mL), the product was obtained as a yellow solid (0.99 g, 85%). ^{1}H NMR (300 MHz, $CDCl_3$): δ 1.24 (t, J = 7.06 Hz, 3 H), 1.47−1.75 (m, 6 H), 1.87 (m, 2 H), 3.37−3.51 (m, 4 H), 4.03 (t, J = 6.12 Hz, 2 H), 6.65 (d, J = 9.12 Hz, 2 H), 6.99 (d, J = 8.86 Hz, 2 H), 7.25−7.52 (m, 23 H), 7.78 (d, J = 9.02 Hz, 2 H), 8.16 (d, J = 7.60 Hz, 4 H). ^{13}C NMR (75 MHz, $CDCl_3$): δ 12.52, 26.23, 27.03, 27.62, 29.51, 45.66, 50.76, 68.16, 110.00, 111.58, 115.28, 115.91, 116.32, 119.11, 119.97, 120.49, 123.41, 123.68, 126.05, 128.14, 128.32, 131.60, 134.26, 140.10, 141.26, 147.19, 152.65, 156.65, 157.91.

4,4′-Di(carbazol-9-yl)-4″-(12-{*N*-ethyl-*N*-[4-(2,2-dicyanovinyl)phenyl]amino}dodecanoxy)triphenylamine, DCST−12C−DCTA (14c). With use of the procedure above and starting with **13c** (4.3 g, 4.7 mmol), malononitrile (0.47 g, 7.1 mmol), acetic acid (0.08 g), and pyridine (20 mL), the product was obtained as a yellow solid (3.8 g, 84%). ^{1}H NMR (300 MHz, $CDCl_3$): δ 1.22 (t, J = 7.20 Hz, 3 H), 1.37 (m, 14 H), 1.54 (m, 2 H), 1.64 (m, 2 H), 1.90 (m, 2 H), 3.35 (t, J = 7.80 Hz, 2 H), 3.45 (q, J = 7.20 Hz, 2 H), 4.03 (t, J = 6.30 Hz, 2 H), 6.63 (d, J = 9.3 Hz, 2 H), 7.01 (d, J = 8.7 Hz, 2 H), 7.25−7.53 (m, 23 H), 7.75 (d, J = 9.3 Hz, 2 H), 8.18 (d, J = 7.8 Hz, 4 H). ^{13}C NMR (75 MHz, $CDCl_3$): δ 12.49, 26.31, 27.20, 27.66, 29.56 (m), 29.60 (m), 29.75 (m), 45.58, 50.84, 68.59, 71.12, 110.04, 111.62, 115.32, 116.07, 116.37, 119.08, 120.01, 120.48, 123.48, 123.71, 126.08, 128.14, 128.32, 131.65, 134.23, 139.99, 141.35, 147.29, 152.79, 156.90, 157.90.

Acknowledgment. Support of this work from U.S. Air Force Office of Scientific Research (Grant Nos. F49620-00-1-0038 and F49620-98-1-0459) is gratefully acknowledged.

CM020702I